Clinical Biomechanics 63 (2019) 134–139

Contents lists available at ScienceDirect

Clinical Biomechanics

journal homepage: www.elsevier.com/locate/clinbiomech

How does a novel knitted titanium nucleus prosthesis change the kinematics of a cervical spine segment? A biomechanical cadaveric study

Patrick Ziegler[a], Hans-Peter Kaps[a], Stephanie Goerke[b], Gauri Tendulkar[a], Alfred Buck sen.[c], Andreas Nuessler[a,*], Werner Schmoelz[d]

[a] *Eberhard Karls Universität Tübingen, Department for Traumatology and Reconstructive Surgery, Siegfried-Weller-Institute for Trauma Research, BG Trauma Center Tubingen, Germany*
[b] *Medical University of Innsbruck, Department of Anatomy, Histology and Embryology, Innsbruck, Austria*
[c] *Buck GmbH and Co.KG, Bondorf, Germany*
[d] *Medical University Innsbruck, Trauma Surgery, Innsbruck, Austria*

ARTICLE INFO

Keywords:
Nucleus prosthesis
Disc replacement
Novel nucleus implant
Disc arthroplasty

ABSTRACT

Background: Total disc replacement is a possible treatment alternative for patients with degenerative disc disease, especially in the cervical spine. The aim is to restore the physiological flexibility and biomechanical behavior. A new approach based on these requirements is the novel nucleus prosthesis made of knitted titanium wires.

Methods: The biomechanical functionalities of eight human cervical (C4-C7) spine segments were investigated. The range of motion was quantified using an ultra-sound based motion analysis system. Moreover, X-rays in full flexion and extension of the segment were taken to define the center of rotation before and after implantation of the nucleus prosthesis as well as during and after complex cyclic loading.

Findings: The mean range of motion of the index segment (C5/6) in flexion/extension showed a significant reduction of range of motion from 9.7° (SD 4.33) to 6.0° (SD 3.97) after implantation ($P = 0.037$). Lateral bending and axial rotation were not significantly reduced after implanting and during cyclic loading in our testing. During cyclic loading the mean range of motion for flexion/extension increased to 7.2° (SD 3.67). The center of rotation remained physiological in the ap-plane and moved cranially in the cc-plane (−27% to −5% in cc height) during the testing.

Interpretation: The biomechanical behavior of the nucleus implant might lower the risk for adjacent joint disorders and restore native function of the index segment. Further in vivo research is needed for other factors, like long-term effects and patient's satisfaction.

1. Introduction

There are evidences of failure of conservative therapies for cervical disc herniation or degenerative disorders, indicating a transition towards surgical treatment of the cervical spine. Most of the currently available surgical treatments reduce the pain but do not restore the mechanical functionality of the spine. It is well known, that adjacent level disorders are possible long-term complications if the biomechanical properties of the spine are not restored (Anderson and Rouleau, 2004; Bertagnoli et al., 2006).

In the majority of surgical treatments, the nucleus of the affected segment is removed, followed by segment fusion (Welke et al., 2016). To preserve mechanical features of the spine, non-fusion implants are gaining much attention in the treatment of painful intervertebral disc or facet joint disorders, trying to mimic the biomechanical behavior of the healthy nucleus (Phillips et al., 2015). There are numerous types of nucleus prostheses and through further research the number will increase (Bartels et al., 2008). Clinical settings (short- and midterm results) do not always meet the expectations, because depending on the used implant they do not exceed those of the "gold standard" of fusion (Shichang et al., 2016; Wachowski et al., 2017). However, recent long-term results of total disc replacement using the Mobi-C© Cervical Disc showed better outcome compared with anterior cervical discectomy and fusion after seven years. > 95% of the patients were "very satisfied" at this point after total disc replacement (Radcliff et al., 2017). McAnany et al. reported that cervical disc replacement is the more cost

* Corresponding author at: Eberhard Karls University Tubingen, BG Trauma Center, Schnarrenbergstr. 95, 72076 Tubingen, Germany.
E-mail address: andreas.nuessler@gmail.com (A. Nuessler).

https://doi.org/10.1016/j.clinbiomech.2019.03.001
Received 12 June 2018; Accepted 4 March 2019

effective procedure after seven years compared to anterior cervical discectomy and fusion (McAnany et al., 2018).

A new technology to preserve the motion of the treated disc as well as its damping properties is a nucleus prosthesis made of knitted titanium filaments (Tendulkar et al., 2016). Because of the rough surface of the prosthesis, the implant migration should be reduced, which remains one of the major problems. Its deformable architecture is designed to restore normal flexibility as the knitted titanium filaments are compressed into the shape of the actual disc requirements (Kettler et al., 2007).

The aim of the present biomechanical cadaver study was to evaluate the effect of the novel knitted nucleus prosthesis on the range of motion (RoM) in the immediate postoperative state as well as after cyclic loading to provoke possible implant subsidence/migration during loading in a human model.

Hypotheses:

1.) The RoM (flexion/extension, lateral bending and axial rotation) of a segment treated with the knitted nucleus replacement differs to the native untreated segment.
2.) The RoM in the treated segment after cyclic loading shows a significant change to the native untreated one and to the immediate post implanted RoM.
3.) The Center of Rotation (CoR) in flexion/extension of a segment treated with the knitted nucleus replacement will not differ significantly from native untreated motion segment.
4.) The knitted nucleus replacement will not dislocate or migrate during cyclic loading.

2. Methods

2.1. Specimens

Eight fresh frozen cervical spine specimens (C4–C7) of 5 female (62.5%) and 3 male (37.4%) donors were used for testing. The age was 70.6 (SD 10.4) years in mean. The bodies were donated by people who had given their informed consent prior to death for their use for scientific and educational purposes (McHanwell et al., 2008). Spinal specimens were stored at −20 °C until test preparation. Prior to preparation the specimens were thawed at 6° for 12 h. Soft tissue was removed, while the osteoligamentous structures were preserved. To prevent desiccation during the preparation and during the testing, the specimens were kept moist with saline solution.

C4 and C7 were embedded in PMMA (Technovit 3040, Heraeus Kulzer GmbH, Wehrheim, Germany). Flanges were fixed to the PMMA blocks for mounting the specimen in the spine tester. Fixation screws for a three dimensional motion analysis system were positioned to the posterior part of the embedding and the spinous process of C5 and C6. Implantations of the prosthesis were carried out on the motion segment C5/6.

2.2. Implants and surgical procedure

Interconnected porous (volumetric porosity 67.67 SD 0.824%, density of 0.75 mg/cm^3) Ti6Al4V scaffolds were fabricated using medical grade titanium alloy (Ti6Al4V) wires with diameter of 0.25 mm and further knitted to produce a mesh like cuboidal disk structure (Buck Co& GmbH, Bondorf, Germany). The scaffolds have been electro-polished to generate smooth wear resistant surface with defined finish (Fig. 1) (Tendulkar et al., 2016). The implants were manufactured according to CT scans of each cadaver spine segment. The segment height of the implants varied from 5 mm to 7 mm and the foot print of the implants varied from 9 × 12 mm to 10.5 × 14 mm. We implanted the prosthesis through an anterior approach. The annulus was fenestrated following a complete removal of the nucleus pulposus as well as the cartilaginous endplates.

Fig. 1. Knitted disc prosthesis for cervical spine made of titanium filaments and pressed into the shape.

2.3. Experimental setup

All flexibility tests were carried out in a six-degree of freedom spine tester, at room temperature. Specimens were loaded with pure moments, applied by a stepper motor to control the loading of the specimens (Disch et al., 2008; Schmoelz et al., 2009; Schmoelz et al., 2017). A six-component load cell (FT Delta 660-60, Schunk Lauffen, Germany) attached to the cranial end of the spine was used for feedback control of the stepper motor, which applied the bending moment. The biomechanical testing of the spines was carried out according to the recommendations for testing of spinal implants (Wilke et al., 1998).

The intersegmental motions of the instrumented levels (C4–C7) were measured using an ultra-sound based three-dimensional motion analysis system (Winbiomechanics, Zebris, Isny, Germany). The flexibility tests were carried out with pure moments of 1.5 Nm (loading rate 0.7°/*sec*, ramp shaped) in the three motion planes (flexion/extension, lateral bending in both sides, axial rotation in both sides) (Hartmann et al., 2015; Koller et al., 2015) (Fig. 2). The recorded load and segmental motions were used to create a load/displacement hysteresis curve and to determine the RoM of the third load cycle (Wilke et al., 1998).

Furthermore, the CoR and implant migration were determined by radiographical images. These were performed in maximum flexion and maximum extension during flexibility testing in the spine tester (Fig. 3). Then, the location of CoRs and the implant position were calculated using an automated clinical method for functional radiographical analysis (FXA; ACES GmbH, Esslingen, Germany). The software matches two images such as vertebral bodies using a 2-d grayscale cross-correlation algorithm that is based on a modified iterative best-fit approach. The location of the CoR in anterior-posterior and cranio-caudal direction was normalized to the size of the caudal vertebra of the motion segment for each specimen. Accuracy and reliability of this method have been previously validated in a separate study for flexion and extension (Schulze et al., 2011). Within the image analysis of the functional X-rays a possible change in the implant position during flexion extension, as well as possible implant migration in the course of cyclic loading was evaluated.

2.4. Cyclic loading

Cyclic loading was applied in a servohydraulic material testing machine (MTS Mini Bionix 858, Eden Prairie, USA), with the specimen rotating around its own axis on a turntable. The cyclic loading was applied eccentric to the rotational axis of the specimen by the piston of the material testing machine (Fig. 4). With the specimen's rotation around its own axis, this results in an axial loading superimposed by a bending moment, which continuously changes its direction (from flexion to right lateral bending to extension to left lateral bending and

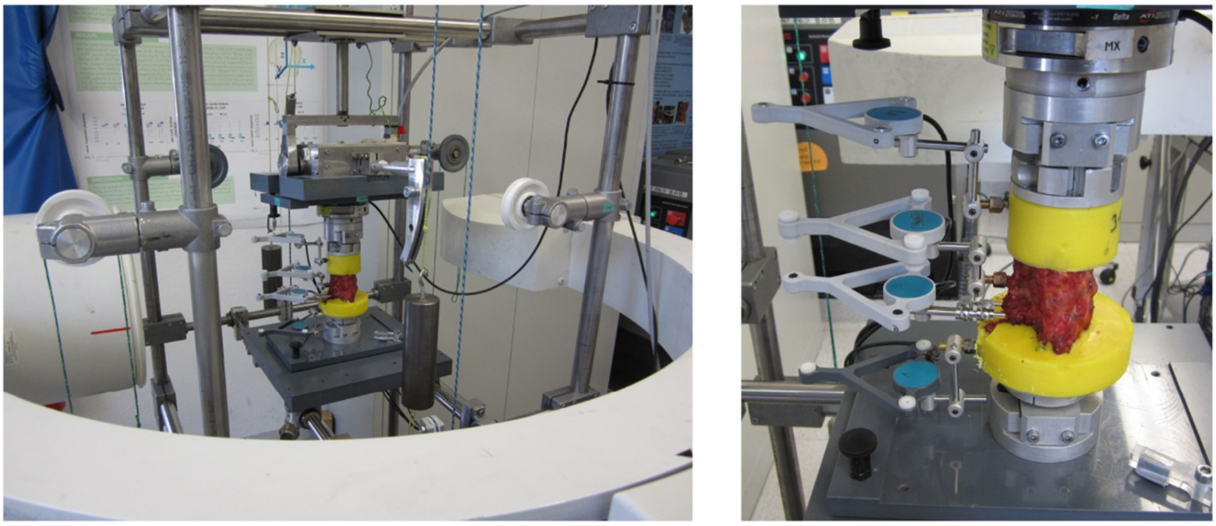

Fig. 2. Test setup with specimen of the presented test series.

back to flexion). The setup was adopted from Wilke et al. (Wilke et al., 2006) and was applied previously in studies conducted in the laboratory (Hartmann et al., 2015; Koller et al., 2015). Briefly, the lever arm for the eccentric loading was set to 1 cm and sinusoidal cyclic loading was applied with 2 Hz while the specimen rotated on a turntable with a rate of 2°/*sec* around the long axis of the specimen (Hartmann et al., 2017). In the first cyclic loading period the magnitude varied between 20 and 150 N and was increased to 20 to 250 N in the second period. The load range was chosen according to previous published studies with comparable setups and loading magnitudes reported by Patwardhan (Hartmann et al., 2017; Koller et al., 2015; Patwardhan et al., 2000). By this, specimens were first loaded for 5000 cycles with a maximum axial load of 150 N (range 20 to 150 N) and a maximum bending moment of 1.5 Nm (range 0.2 to 1 .5Nm) followed by another 5000 cycles with a maximum axial load of 250 N and a maximum bending moment 2.5 Nm (range 0.2 to 2 .5Nm).

Test conditions:

1. Flexibility test of native cervical spine
2. Flexibility test with implanted nucleus prosthesis
3. Cyclic loading – 1st cyclic loading period (5000 cycles 20–150 N)
4. Flexibility test with implanted nucleus prosthesis – after 1st cyclic loading interval
5. Cyclic loading – 2nd cyclic loading period (5000 cycles 20–250 N)
6. Flexibility test with implanted nucleus prosthesis – after 2nd cyclic loading interval

2.5. Statistical analysis

Statistical Analysis of the RoM was carried out using the SPSS (version 24) software. Distribution of the data was evaluated with the Shapiro-Wilk test. For statistical comparison of normally distributed data a General Linear Model (GLM) with repeated measures was carried out to compare the main effects and *P*-values were adjusted for multiple corrections according to Bonferroni. The level of significance was accepted at $\alpha < 0.05$ in the evaluation of the results.

3. Results

In general, with the implantation of the knitted nucleus prostheses a reduction in RoM in flexion/extension in the index segment C5/6 was observed. In the course of cyclic loading the RoM remained stable in the specimens.

The mean RoM of C5/6 to the native state in flexion/extension, showed a significant decrease from 9.7° (SD 4.33) to 6.0° (SD 3.97) after implantation ($P < 0.037$). During cyclic loading the mean RoM

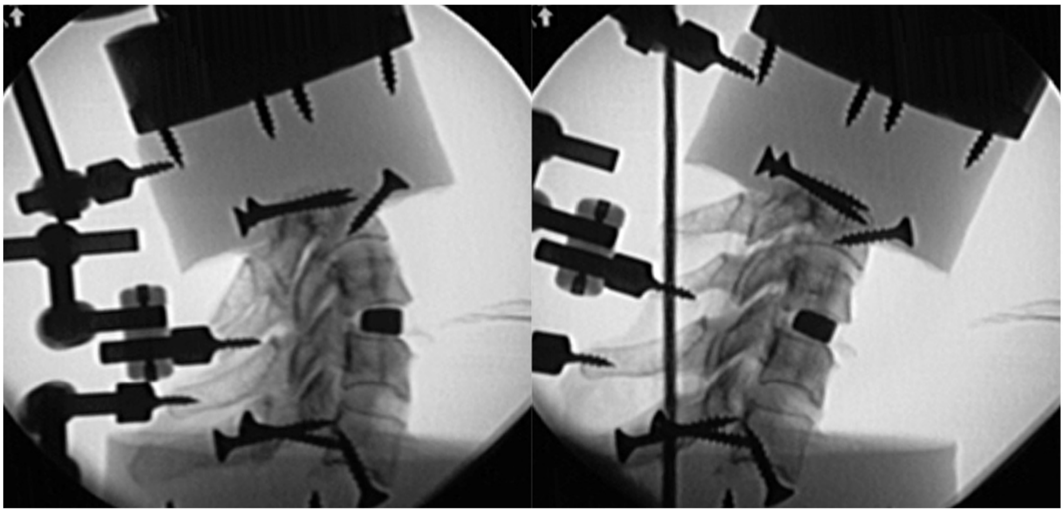

Fig. 3. Radiographs in maximum flexion and maximum extension in the post implanted state.

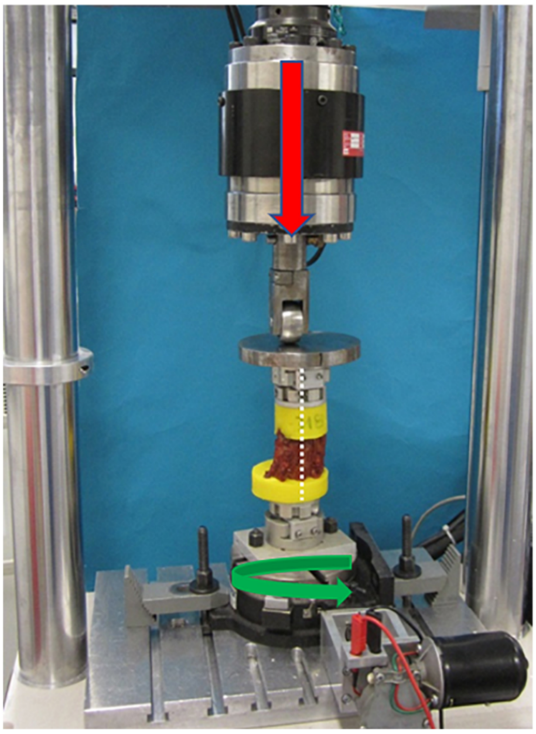

Fig. 4. The red arrow indicates static load vector of the applied cyclic loading. The green arrow indicates counterclockwise rotation of the specimens on the turntable with the white dashed line showing the rotational axis of the specimen. By the offset of the static load vector to the rotational axis of the specimen an axial load and a constantly changing bending moment (flexion to right lateral bending to extension to left lateral bending and back to flexion) are applied. (For interpretation of the references to colour in this figure legend, the reader is referred to the web version of this article.)

Table 1
Range of motion of the index segment in native state, after implantation and after cyclic loading. $^*P = 0.037$ for flexion extension in native state compared to implantation before cyclic loading.

	Lateral bending C5/6 in degrees	Flexion extension C5/6 in degrees	Axial rotation C5/6 in degrees	$P < 0.05$
Native	4.3 (SD 2.37)	9,7 (SD 4.33)	4.1 (SD 2.14)	
Implanted	3.2 (SD 2.75)	6.0 (SD 3.97)	3.3 (SD 2.27)	0.037* (flexion extension)
Cyclic 1	3.6 (SD 3.13)	6.9 (SD 3.94)	3.5 (SD 2.56)	
Cyclic 2	3.6 (SD 3.0)	7.2 (SD 3.67)	3.4 (SD 2.48)	

increased to 6.9° (SD 3.94) and finally to 7.2° (SD 3.67) (Fig. 3, Table 1). Compared to the native state the adjacent segments showed a small increase in RoM after implantation and in the course of cyclic loading for flexion/extension (Table 2).

We also observed a reduction in RoM in lateral bending in the index segment C5/6 after implantation of the knitted nucleus prosthesis. Comparing the mean RoM of C5/6 to the native state we found a small reduction of RoM from 4.3° (SD 2.37) to 3.2° (SD 2.75) after implantation ($P = 0.483$). After the first cyclic loading the mean RoM in lateral bending increased to 3.6° (SD 3.13). After the second cyclic loading the mean RoM remained at 3.6° (SD 3.0). Compared to the native state, the reduction of RoM did not show any significant differences (Fig. 3, Table 1). Compared to the native state the adjacent segments showed a small, non-significant increase in RoM after implantation and in the course of cyclic loading for lateral bending (Table 2).

Regarding the axial rotation in the index segment C5/6 we observed a small reduction of the RoM after implantation of the knitted nucleus replacement. The mean RoM of C5/6 was reduced after implantation of the knitted nuclei replacement compared to the native state from 4.1° (SD 2.14) to 3.3° (SD 2.27) ($P = 0.215$). In the course of cyclic loading the mean RoM increased to 3.5° (SD 2.56) and remained stable at 3.4° (SD 2.48) after the cyclic loading. We couldn't detect a significant change in RoM for axial rotation in our study set up. (Fig. 5, Table 1).

The CoR of the native C5/6 segment was detected in the center of the vertebral body, in anterior-posterior direction at 44% of the vertebral AP length and in cranio-caudal direction at −27% of the vertebral CC height (Fig. 6). With the implantation of the nucleus replacement the location of the CoR moved cranially to the superior endplate of the lower vertebra at −5.5% of the vertebral CC height. During cyclic loading the CoR moved further caudal to +4.5% of vertebral CC height. In the anterior posterior direction, a marginal shift of the CoR from 44% in the native state to 34.5% in the implanted state and 42.5% after cyclic loading was observed (Fig. 6). No implant migration was observed during the study.

After the testing protocol of the study we dissected the specimens and removed the nucleus implant. After removing the implant, we inspected the implant's filaments and the endplates of the index segment. We could detect a small indentation in the shape of the implant but no further harm to the endplates. The implants didn't show any broken filaments or macroscopic differences in shape.

4. Discussion

Titanium is a common material for biomedical implants because of its mechanical properties, biocompatibility and low immunogenicity (Li et al., 2014). Compared to traditional metallic materials, novel strategy of pursuing knitted geometry in this study upholds an ability to restore and maintain the flexibility, height of the affected segment and migration resistance, flexibility maintenance. Since the first biomechanical study in a bovine specimen by Kettler et al. in 2007, numerous

Table 2
Range of motion of the adjacent segments (C4/5 and C6/7) in native state, after implantation and after cyclic loading.

	Lateral bending in degrees (C4/5)	Lateral bending in degrees (C6/7)	Flexion Extension in degrees (C4/5)	Flexion Extension in degrees (C6/7)	Axial rotation in degrees (C4/5)	Axial rotation in degrees (C6/7)
Native	7.0 (SD 2.47)	4.1 (SD 2.09)	11.7 (SD 3.90)	8.6 (SD 4.36)	7.1 (SD 2.13)	3.1 (SD 1.61)
Implanted	7.3 (SD 2.84)	4.1 (SD 2.1)	13.3 (SD 5.00)	9.32 (SD 4.88)	7.4 (SD 1.87)	3.7 (SD 1.79)
Cyclic 1	7.8 (SD 3.26)	4.6 (SD 2.42)	14.1 (SD 4.57)	10.0 (SD 5.11)	7.8 (SD 2.17)	3.9 (SD 2.06)
Cyclic 2	7.9 (SD 3.41)	4.9 (SD 2.66)	15.3 (SD 5.59)	10.4 (SD 5.22)	7.9 (SD 2.18)	4.0 (SD 1.97)

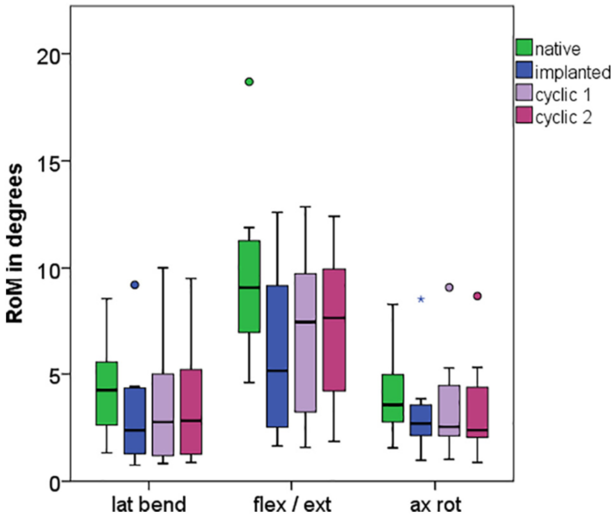

Fig. 5. Boxplot showing the median and 25% and 75% quartiles of the index segment C5/6 in degrees.

improvements like electro-polishing and using new different titantium filaments have been accomplished (Kettler et al., 2007). Besides testing the new implant in human spine for the first time we also performed X-ray based analysis of the CoR.

The gold standard in treatment of degenerative disc disease in the cervical spine is still the discectomy and the fusion of the segment. However, clinical long-term studies have shown evidence of an increased incidence of pathologies in the motion segments adjacent the fused segment (Anderson and Rouleau, 2004; Bertagnoli et al., 2006). Chung et al. found adjacent level pathologies in over 92% of the patients after fusion based on the theory of increased degeneration of the adjacent segments by increased mobility (Chung et al., 2014). Moreover, different types of prosthesis, which are currently used, show similar problems. Adjacent joint disorders are seen up to 6% after implanting the Bryan cervical disc prosthesis following Dejaegher et al. (Dejaegher et al., 2017). These problems might be reduced by physiological movements in the index segment. The adjacent segments didn't show significant differences in RoM after implanting the nucleus prothesis or after cyclic loading in our study. In general, our measurements of RoM of the adjacent levels are comparable with studies by Anderst et al. They could state that the segment C4/5 showed higher RoMs than C6/7 in all dimensions in native cervical spines and after segmental fusion (Anderst et al., 2013; Anderst et al., 2015).

In our biomechanical set up, RoM was reduced in all dimensions. Yet, this reduction was not significant except for flexion/extension. However, due to the small sample size of the study, the significances need to be interpreted critically. The identified RoM after cycling loading showed even closer results to the RoM of the native segment. Similar results were reported by Dmitirev et al., investigating the PCM disc arthroplasty (Dmitriev et al., 2005). An increase of RoM after implanting a cervical disc prosthesis in vitro was stated by DiAngelo et al. (DiAngelo et al., 2004). These authors concluded that the use of a prosthetic total disc replacement device, such as the ProDisc-C, to treat symptomatic degenerative cervical disc disease may minimize or alleviate the adjacent-segment disease associated with fusion surgery. However, Lou et al. found a significant forward shift of CoR after implantation of the ProDisc-C prosthesis in 23 patients (Lou et al., 2016). Ryu et al. investigated the Bryan cervical disc prosthesis and reported from a non-significant change in of CoR after surgery or over the course of follow-up (5 years) (Ryu et al., 2013). These findings go along with the results we could state by investigating the knitted nucleus prothesis.

The implant couldn't reach the native RoM in our study completely, although it showed an increase of RoM during the testing. We believe that the increase of RoM after cyclic loading is based on the anchoring of the knitted titanium implant onto the bone surface, which shows its real dampening characters after cyclic loading. Moreover, the increasing RoM might be based on an initial adjustment of the implant to the vertebral body geometry that results in the RoM remaining constant. In the course of our study we didn't observe any migration of the nucleus replacement in the eight specimens, even though the annulus could not be closed after fenestration of the disc and application of stringent loading conditions.

The compressive force during cyclic loading was intended as axial preload, which is acting on the human cervical spine depending on a lying-down (20 N) or standing (250 N) position (Patwardhan et al., 2000). The bending moment we used in our study was up to 2.5 Nm. This could be reached by a 10 mm lever arm which applied the force eccentrically on the specimens. This is the highest bending moment recommended in the literature for testing of the cervical spine (Wilke et al., 1998). Therefore, we expect our implant to show good primary stability; otherwise it should have migrated under these loading conditions. Based on the radiological data we couldn't state any implant

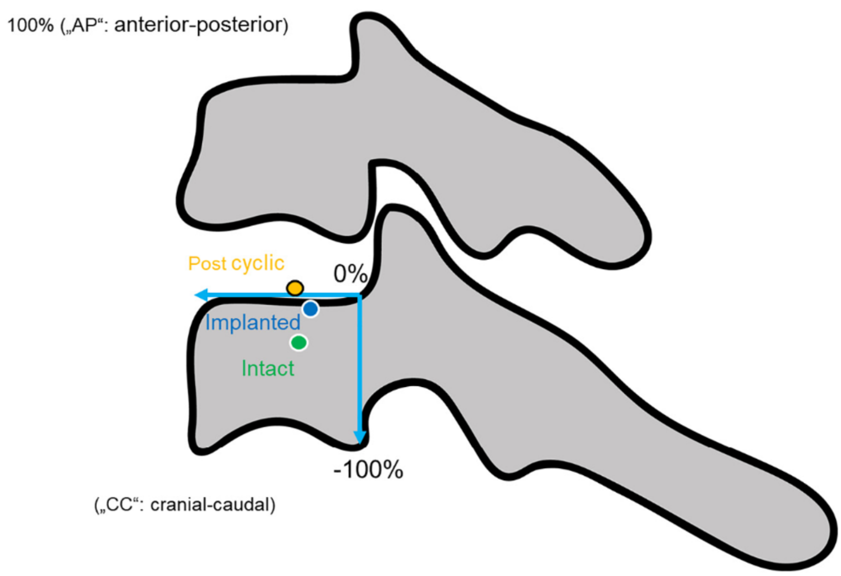

Fig. 6. Visualization of the CoR in intact condition, after implantation of the knitted titanium implant and after cyclic loading.

migration either. The knitted titanium filaments built a rough surface, which is supposed to prevent migration, and at the same time it mimics the biomechanical behavior of the native nucleus. Several nucleus implants showed migration and therefore change the biomechanical behavior while physiological testing (Anderson et al., 2017). Therefore, we think, that more loading won't change the biomechanical behavior of the knitted nucleus implant. The surface prevents the implant of migration or extrusion. However, it is important to create a fitting cavity, not larger than the implant, as otherwise the implant's shape won't adjust properly to the vertebral body geometry. Besides the size of the cavity, individualized endplate preparation may also be considered in implant anchorage since patient's vertebral surfaces show individual differences. After the implantation, the CoR stayed physiological in the anterior-posterior plane. In the cranial-caudal direction, the CoR moves towards the cranial endplate. This is understandable, since the shift of the CoR towards the implant reduces the a-p translation of the two vertebral bodies, too. Limitations might be future issues of the presented nucleus implant with heterotopic ossifications and following spontaneous fusion of the segment. If secondary surgery is needed, the damage to the segment might be reduced due to the small implant size and because the annulus is left in place.

5. Conclusion

The results of this study showed promising data for the tested nucleus implant made of knitted titanium filaments. The fact that the implant mimics the biomechanical properties of the native segment might lower the risk for adjacent joint disorders and restore native function. However, as this is a cadaver study with limited sample size these hypotheses must be tested in long-term studies.

Author contributions statement

Study designed and initiated by PZ, AN and WS. Interpretation, statistics and writing of the paper by PZ, WS, and AN. Experiment and data collection by HPK, PZ, SG, and WS.

Revising manuscript by PZ, WS, AN, GT, HPK, SG and AB.

All authors read and approved the final manuscript.

Conflict of interest

The authors declare that they have no conflict of interest.

Acknowledgement

The work was partially supported by theGerman Federal Ministry for Economic Affairs and Energy - Zentrales Innovations program-KF3010902AJ4. We further acknowledge the support by the Deutsche Forschungsgemeinschaft and Open Access Publishing Fund of University of Tübingen.

References

Anderson, P.A., Rouleau, J.P., 2004. Intervertebral disc arthroplasty. Spine 29, 2779–2786.
Anderson, P.A., Nassr, A., Currier, B.L., Sebastian, A.S., Arnold, P.M., Fehlings, M.G., Mroz, T.E., Riew, K.D., 2017. Evaluation of adverse events in Total disc replacement: a meta-analysis of FDA summary of safety and effectiveness data. Glob. Spine J. 7, 76S–83S.
Anderst, W.J., Lee, J.Y., Donaldson 3rd, W.F., Kang, J.D., 2013. Six-degrees-of-freedom cervical spine range of motion during dynamic flexion-extension after single-level anterior arthrodesis: comparison with asymptomatic control subjects. J. Bone Joint Surg. 95, 497–506.
Anderst, W.J., Donaldson 3rd, W.F., Lee, J.Y., Kang, J.D., 2015. Three-dimensional intervertebral kinematics in the healthy young adult cervical spine during dynamic functional loading. J. Biomech. 48, 1286–1293.
Bartels, R.H., Donk, R.D., Pavlov, P., van Limbeek, J., 2008. Comparison of biomechanical properties of cervical artificial disc prosthesis: a review. Clin. Neurol. Neurosurg. 110, 963–967.
Bertagnoli, R., Yue, J.J., Fenk-Mayer, A., Eerulkar, J., Emerson, J.W., 2006. Treatment of symptomatic adjacent-segment degeneration after lumbar fusion with total disc arthroplasty by using the prodisc prosthesis: a prospective study with 2-year minimum follow up. J. Neurosurg. Spine 4, 91–97.
Chung, J.Y., Kim, S.K., Jung, S.T., Lee, K.B., 2014. Clinical adjacent-segment pathology after anterior cervical discectomy and fusion: results after a minimum of 10-year follow-up. Spine J. 14, 2290–2298.
Dejaegher, J., Walraevens, J., van Loon, J., Van Calenbergh, F., Demaerel, P., Goffin, J., 2017. 10-Year follow-up after implantation of the Bryan cervical disc prosthesis. Eur. Spine J. 26, 1191–1198.
DiAngelo, D.J., Foley, K.T., Morrow, B.R., Schwab, J.S., Song, J., German, J.W., Blair, E., 2004. In vitro biomechanics of cervical disc arthroplasty with the ProDisc-C total disc implant. Neurosurg. Focus. 17, E7.
Disch, A.C., Schaser, K.D., Melcher, I., Luzzati, A., Feraboli, F., Schmoelz, W., 2008. En bloc spondylectomy reconstructions in a biomechanical in-vitro study. Eur. Spine J. 17, 715–725.
Dmitriev, A.E., Cunningham, B.W., Hu, N., Sell, G., Vigna, F., McAfee, P.C., 2005. Adjacent level intradiscal pressure and segmental kinematics following a cervical total disc arthroplasty: an in vitro human cadaveric model. Spine 30, 1165–1172.
Hartmann, S., Thome, C., Keiler, A., Fritsch, H., Hegewald, A.A., Schmolz, W., 2015. Biomechanical testing of circumferential instrumentation after cervical multilevel corpectomy. Eur. Spine J. 24, 2788–2798.
Hartmann, S., Thome, C., Tschugg, A., Paesold, J., Kavakebi, P., Schmolz, W., 2017. Cement-augmented screws in a cervical two-level corpectomy with anterior titanium mesh cage reconstruction: a biomechanical study. Eur. Spine J. 26, 1047–1057.
Kettler, A., Kaps, H.P., Haegele, B., Wilke, H.J., 2007. Biomechanical behavior of a new nucleus prosthesis made of knitted titanium filaments. SAS J. 1, 125–130.
Koller, H., Schmoelz, W., Zenner, J., Auffarth, A., Resch, H., Hitzl, W., Malekzadeh, D., Ernstbrunner, L., Blocher, M., Mayer, M., 2015. Construct stability of an instrumented 2-level cervical corpectomy model following fatigue testing: biomechanical comparison of circumferential antero-posterior instrumentation versus a novel anterior-only transpedicular screw-plate fixation technique. Eur. Spine J. 24, 2848–2856.
Li, Y., Yang, C., Zhao, H., Qu, S., Li, X., Li, Y., 2014. New developments of Ti-based alloys for biomedical applications. Materials 7, 1709–1800.
Lou, J., Li, H., Rong, X., Wu, W., Liu, H., 2016. Location change of center of rotation after single-level cervical total disc replacement with ProDisc-C. Acta Orthop. Traumatol. Turc. 50, 339–345.
McAnany, S.J., Merrill, R.K., Overley, S.C., Kim, J.S., Brochin, R.L., Qureshi, S.A., 2018. Investigating the 7-year cost-effectiveness of single-level cervical disc replacement compared to anterior cervical discectomy and fusion. Glob. Spine J. 8, 32–39.
McHanwell, S.B.E., Chirculescu, A.R.M., Drukker, J., van Mameren, H., Mazzotti, G., Pais, D., Paulsen, F., Plaisant, O., Caillaud, M.M., Laforet, E., Riedere, B.M., Sanudo, J.R., Bueno-Lopez, J.L., Donate-Oliver, F., Sprumont, P., Teofilovski-Parapid, G., Moxham, B.J., 2008. The legal and ethical framework governing body donation in Europe - a review of current practice and recommendations for good practice. Eur. J. Anat. 12, 1–24.
Patwardhan, A.G., Havey, R.M., Ghanayem, A.J., Diener, H., Meade, K.P., Dunlap, B., Hodges, S.D., 2000. Load-carrying capacity of the human cervical spine in compression is increased under a follower load. Spine 25, 1548–1554.
Phillips, F.M., Geisler, F.H., Gilder, K.M., Reah, C., Howell, K.M., McAfee, P.C., 2015. Long-term outcomes of the US FDA IDE prospective, randomized controlled clinical trial comparing PCM cervical disc arthroplasty with anterior cervical discectomy and fusion. Spine 40, 674–683.
Radcliff, K., Davis, R.J., Hisey, M.S., Nunley, P.D., Hoffman, G.A., Jackson, R.J., Bae, H.W., Albert, T., Coric, D., 2017. Long-term evaluation of cervical disc arthroplasty with the Mobi-C(c) cervical disc: a randomized, prospective, multicenter clinical trial with seven-year follow-up. Int. J. Spine Surg. 11, 31.
Ryu, W.H., Kowalczyk, I., Duggal, N., 2013. Long-term kinematic analysis of cervical spine after single-level implantation of Bryan cervical disc prosthesis. Spine J. 13, 628–634.
Schmoelz, W., Onder, U., Martin, A., von Strempel, A., 2009. Non-fusion instrumentation of the lumbar spine with a hinged pedicle screw rod system: an in vitro experiment. Eur. Spine J. 18, 1478–1485.
Schmoelz, W., Sandriesser, S., Loebl, O., Bauer, M., Krappinger, D., 2017. Effect of cage design, supplemental posterior instrumentation and approach on primary stability of a lumbar interbody fusion - a biomechanical in vitro study. Clin. Biomech. 48, 30–34.
Schulze, M., Trautwein, F., Vordemvenne, T., Raschke, M., Heuer, F., 2011. A method to perform spinal motion analysis from functional X-ray images. J. Biomech. 44, 1740–1746.
Shichang, L., Yueming, S., Limin, L., Lei, W., Zhongjie, Z., Chunguang, Z., Xi, Y., 2016. Clinical and radiologic comparison of dynamic cervical implant arthroplasty and cervical total disc replacement for single-level cervical degenerative disc disease. J. Clin. Neurosci. 27, 102–109.
Tendulkar, G., Grau, P., Ziegler, P., Buck Sr., A., Buck Jr., A., Badke, A., Kaps, H.P., Ehnert, S., Nussler, A.K., 2016. Imaging cell viability on non-transparent scaffolds - using the example of a novel knitted titanium implant. J. Vis. Exp.
Wachowski, M.M., Weiland, J., Wagner, M., Gezzi, R., Kubein-Meesenburg, D., Nagerl, H., 2017. Kinematics of cervical segments C5/C6 in axial rotation before and after total disc arthroplasty. Eur. Spine J. 26 (9), 2425–2433.
Welke, B., Schwarze, M., Hurschler, C., Book, T., Magdu, S., Daentzer, D., 2016. In vitro investigation of a new dynamic cervical implant: comparison to spinal fusion and total disc replacement. Eur. Spine J. 25, 2247–2254.
Wilke, H.J., Wenger, K., Claes, L., 1998. Testing criteria for spinal implants: recommendations for the standardization of in vitro stability testing of spinal implants. Eur. Spine J. 7, 148–154.
Wilke, H.J., Mehnert, U., Claes, L.E., Bierschneider, M.M., Jaksche, H., Boszczyk, B.M., 2006. Biomechanical evaluation of vertebroplasty and kyphoplasty with polymethyl methacrylate or calcium phosphate cement under cyclic loading. Spine 31, 2934–2941.